Journal of the Operational Research Society (2017) 68, 1470–1481

www.palgrave.com/journals

An efficient approximate solution for stochastic Lanchester models

Donghyun Kim[1], Hyungil Moon[1], Donghyun Park[1] and Hayong Shin[1]*

[1]*Industrial and Systems Engineering, KAIST, E2-2 IE Building #3106, KAIST 291, Daehak-ro, Yuseong-gu, Daejeon 34141, South Korea*

Combat modeling is one of the essential topics for military decision making. The Lanchester equation is a classic method for modeling warfare, and many variations have extended its limitations and relaxed its assumptions. As a model becomes more complex, solving it analytically becomes intractable or computationally expensive. Hence, we propose two approximation methods: moment-matching scheme and a supporting method called battle-end approximation. These methods give an approximate solution in a short amount of time, while maintaining a high level of accuracy in simulation results in terms of hypothesis testing and numerical verification. They can be applied to computationally intensive problems, such as optimal resource allocation and analysis with asymmetric power like snipers or stealth aircrafts.

Journal of the Operational Research Society (2017) **68(11),** 1470–1481. doi:10.1057/s41274-016-0163-6; published online 9 February 2017

Keywords: Military; stochastic Lanchester model; Gaussian approximation

1. Introduction

Combat modeling is a fundamental area in the military research that supports strategic decision making such as optimal allocation of resources in warfare. However, modeling warfare is not trivial; it is complex in terms of its variety of factors such as landscape, number of troops, composition of troops, mutual interaction between soldiers. Lanchester (1916) proposed a formal combat modeling scheme with a simple and clear differential equation between two homogeneously armed forces:

$$\frac{dB_t}{dt} = -rR_t \tag{1}$$

$$\frac{dR_t}{dt} = -bB_t \tag{2}$$

where B_t and R_t denote the strengths of each force at time t, while r and b are the corresponding attrition rates. The effect of the landscape or the mutual interactions between soldiers is reflected in the attrition rates of the equation.

Several variations have appeared since Lanchester (1916) introduced his modeling scheme in order to extend its limitations and relax its assumptions. Since it is not appropriate to express all the situations in a war with the constant parameters, there are two different mainstreams of extension.

First, many studies have increased the sophistication of the Lanchester model in deterministic setting. Bracken (1995) developed a generalized homogeneous Lanchester model using exponential index numbers to accommodate the Lanchester's square and linear law. They also empirically validated the model with the Ardennes Campaign of World War II. Hughes (1995) modified the original Lanchester equation and proposed a new model called the "salvo combat model" to describe modern missile warfare; this model includes defensive firepower effects and uses discrete salvos of missiles. Kaup *et al* (2005) suggested the (n, 1) mixed forces model, which involves combat between n-type heterogeneous forces and a homogeneous force. MacKay (2009) extended the (m, 1) mixed forces model to the (m, n) mixed forces model, where each force consists of m (or n) types of heterogeneous forces; this paper also includes the optimal target allocation problem.

Since the original Lanchester equation is deterministic, it cannot represent any random consequences. Second line of extension to the original Lanchester model is to add stochasticity in order to include uncertainty. The main difference of a stochastic Lanchester model is that it incorporates the uncertainty in the attrition rates or target detection probabilities using random variables. Taylor (1980) showed that a stochastic Lanchester equation can be represented as a Markov model. Lappi *et al* (2012) also suggested a dynamical Markovian method of the battle similar to the model of Taylor (1980). They developed a computationally lighter model to predict only the outcome of battle, such as the winning probability of blue forces, without calculating the

*Correspondence: Hayong Shin, Industrial and Systems Engineering, KAIST, E2-2 IE Building #3106, KAIST 291, Daehak-ro, Yuseong-gu, Daejeon 34141, South Korea.
E-mail: hyshin@kaist.ac.kr

joint distribution of the forces during warfare. Amacher and Mandallaz (1986) represented the attrition rates by using Brownian motion for the kill rate rather than using constants. Karmeshu and Jaiswal (1986) considered environmental randomness by treating the kill rate as a random variable that contains dichotomous variables with a possible value of +1 or −1. Armstrong (2005) developed a stochastic version of the salvo combat model of Hughes (1995) with a probabilistic variation in the damage caused by each hit and the probability of success of each attack.

These elaborated Lanchester equations have enabled more precise representations than the original modeling scheme. However, as a model becomes more complex, it becomes intractable to solve analytically; thus, it requires heavy numerical computations. Computational cost explodes when applying stochastic model to (m, n) mixed forces.

In this paper, we propose a new stochastic Lanchester-type equation that was derived directly from the Markov model of Taylor (1980). Taylor defined all the possible outcomes as the states of the Markov model and assumed that there are three possible outcomes after transition: 1 blue decreases, 1 red decreases, or no change. We reformulated this model as stochastic difference equations with Bernoulli random variables, the probability of which depends on the attrition rate and the strength of the opponents. We also present two approximation algorithms. The first is called the moment-matching scheme, which can be widely used for any other stochastic Lanchester equations. The second one is the battle-end approximation, which handles the situation when the forces go to 0. These give not only the approximated joint distribution of large heterogeneous forces, but also the battle-end state distribution of each force. With the proposed approximation, stochastic mixed force models can be solved efficiently.

In the next section, we present our main concept, the moment-matching scheme, and numerical results. We also propose a supporting approximation method called the battle-end approximation, which handles the situation when the forces go to 0. Finally, we suggest some applications to which these methods can be effectively applied.

2. Moment-matching scheme

In this paper, we develop a new but familiar form of stochastic Lanchester-type equation modeled after Taylor (1980). The proposed model follows difference equations:

$$B_{t+\mathrm{d}t} - B_t = -\mathrm{Bern}(rR_t\mathrm{d}t) \tag{3}$$

$$R_{t+\mathrm{d}t} - R_t = -\mathrm{Bern}(bB_t\mathrm{d}t) \tag{4}$$

where $\mathrm{Bern}(p)$ is a Bernoulli random variable with a probability p, while b and r are positive constants that denote the attrition rates. B_t and R_t denote the strengths of blue and red forces at time t. These equations mean that in a small amount of time $\mathrm{d}t$, 1 unit of a force's strength is decreased by a probability that depends on the opposite side's strength. Taylor assumed that there are three possible outcomes after transition: 1 blue decreases, 1 red decreases, or no change. The proposed model assumes one more possible outcome: both decrease.

Like any other complex stochastic differential equation, the suggested difference equations are also hard to solve analytically when $\mathrm{d}t$ goes to 0. There are two ways to solve such stochastic problems. On the one hand, the Monte Carlo simulation method is widely used; it discretizes the model with a small time fraction and generates paths for various scenarios. Even though this method is powerful and has been heavily used for several decades in various fields, it is computationally expensive, especially in our case when the forces become heterogeneous and the time fraction gets smaller. Moreover, it gets harder to get information as forces become large and complex because $\mathrm{d}t$ should be small enough to make a parameter of Bernoulli random variables less than 1 in Eqs. (3) and (4). As $\mathrm{d}t$ gets smaller, the computational cost of the Monte Carlo simulation method grows exponentially. On the other hand, one can use the Markov model, which requires reformulating the original stochastic equation in a Markovian form. Every possible circumstance during the battle is defined as a state (B, R), where B and R are nonnegative integers, denoting the strength of each blue and red force. As in Taylor (1980), there are three possible state transitions for each Δt. If (B, R) is the current state, it will transit to $(B-1, R)$ w.p. $rR\Delta t$, $(B, R-1)$ w.p. $bB\Delta t$, and (B, R) itself w.p. $1 - rR\Delta t - bB\Delta t$. The number of states in this model grows exponentially as the dimension grows. In the mixed force cases, the number of component types determines the dimension, and dimension of 10 or more is common in practice. In such cases, the above Markov model easily goes beyond the computational budget even with modern computing hardware. Hence, we propose approximation methods. We will start with homogeneous forces (of 2 dimension) first, and then the result will be extended (M, N) mixed forces (of $M + N$ dimension).

The key difference between deterministic and stochastic models is their types of solutions. A deterministic model gives a unique point at time t, whereas a stochastic model gives the joint distribution of the forces at time t. Since the direct estimation of the joint distribution from the equation is challenging, we use the *moments* of each force to define the properties of distribution. Preliminary observations using Monte Carlo simulation of the proposed model showed that the joint distribution is unimodal and bell shaped; therefore, we approximate the joint distribution as multivariate Gaussian. Justification for the Gaussian assumption will be discussed at the end of the next section, *Battle-end approximation*. Gaussian distribution is uniquely defined by its mean and variance; hence, only the first and second

moments are sufficient to characterize the distribution. The first and second moments at time $t + \mathrm{d}t$ given the moments at time t are:

$$\mathrm{E}[B_{t+\mathrm{d}t}] = \mathrm{E}[B_t] - r\mathrm{E}[R_t]\mathrm{d}t \tag{5}$$

$$\mathrm{E}[R_{t+\mathrm{d}t}] = \mathrm{E}[R_t] - b\mathrm{E}[B_t]\mathrm{d}t \tag{6}$$

$$\mathrm{E}\left[B_{t+\mathrm{d}t}^2\right] = \mathrm{E}\left[B_t^2\right] - 2r\mathrm{E}[B_tR_t]\mathrm{d}t + r\mathrm{E}[R_t]\mathrm{d}t \tag{7}$$

$$\mathrm{E}\left[R_{t+\mathrm{d}t}^2\right] = \mathrm{E}\left[R_t^2\right] - 2b\mathrm{E}[B_tR_t]\mathrm{d}t + b\mathrm{E}[B_t]\mathrm{d}t \tag{8}$$

$$\begin{aligned}\mathrm{E}[B_{t+\mathrm{d}t}R_{t+\mathrm{d}t}] = \mathrm{E}[B_tR_t] - b\mathrm{E}\left[B_t^2\right]\mathrm{d}t - r\mathrm{E}\left[R_t^2\right]\mathrm{d}t \\ + rb\mathrm{E}[B_tR_t]\mathrm{d}t^2\end{aligned} \tag{9}$$

We define a moment vector M_t as

$$M_t = \left(\mathrm{E}[B_t], \mathrm{E}[R_t], \mathrm{E}\left[B_t^2\right], \mathrm{E}\left[R_t^2\right], \mathrm{E}[B_tR_t]\right)^T$$

where the notation $(\,)^T$ is the transpose of a matrix. Then, Eqs. (5)–(9) can be rewritten as:

$$M_{t+\mathrm{d}t} = (I_5 + V\mathrm{d}t)M_t + o\left(\mathrm{d}t^2\right)K \tag{10}$$

$$V = \begin{pmatrix} 0 & -r & 0 & 0 & 0 \\ -b & 0 & 0 & 0 & 0 \\ 0 & a & 0 & 0 & -2r \\ b & 0 & 0 & 0 & -2b \\ 0 & 0 & -b & -r & 0 \end{pmatrix}, \quad K = \begin{pmatrix} 0 \\ 0 \\ 0 \\ 0 \\ br\mathrm{E}[B_tR_t] \end{pmatrix}$$

where I_5 is the 5×5 identity matrix. The detailed derivation of Eqs. (7)–(9) is in Appendix 1.

Equation (10) shows that the moment vector at time $t + \mathrm{d}t, M_{t+\mathrm{d}t}$ can be calculated from M_t. Since as $\mathrm{d}t \to 0$, $o(\mathrm{d}t^2)$ becomes 0, the following equation holds:

$$M_t = expm(V)^t M_0 \tag{11}$$

where *expm* is the exponential operator for a matrix. Equation (11) means that the first and second moments at arbitrary time t can be derived from the initial moments directly. The matrix exponential is easily computable using the eigendecomposition, so its mean and covariance at time t are also easily derived from the initial moments.

Many combat models that have difference equations can be solved similarly as (11) with a proper matrix V. The strength of the difference Eqs. (3) and (4) is that a heterogeneous case can be modeled and solved in a similar manner. Equations (3) and (4) can be expanded to a heterogeneous case as follows:

$$B_{i,t+\mathrm{d}t} - B_{i,t} = -\mathrm{Bern}\left(\sum_{k=1}^{N} r_{ki}R_{k,t}\mathrm{d}t\right) \quad \forall i = 1\ldots M \tag{12}$$

$$R_{j,t+\mathrm{d}t} - R_{j,t} = -\mathrm{Bern}\left(\sum_{l=1}^{M} b_{lj}B_{l,t}\mathrm{d}t\right) \quad \forall j = 1\ldots N \tag{13}$$

Here, $B_{i,t}\left(R_{j,t}\right)$ denotes the strength of type i (type j) component of blue (red) force at time t. As previously mentioned, the simulation cost for computing the heterogeneously armed case is higher and more time-consuming than that of a homogeneous case. However, since we are assuming that the joint distribution is Gaussian in this scheme, it becomes straightforward to get the joint distribution for the heterogeneously armed force case. Equations (12) and (13) show the combat situation with M-type of blue forces and N-type of red forces. For example, if forces are composed of tanks, infantry, and artillery, these are called 3-type heterogeneous forces. r_{ki} is the attrition rate for an ith type of blue force being attacked by a kth type of red force. Similarly, b_{lj} is the attrition rate for a jth type of red force being attacked by an lth type of blue force. These attrition rate coefficients implicitly contain the fire allocation terms for how to distribute the total fire. However, in this paper we assume fire allocation to be fixed. Estimating the coefficients will be discussed in the conclusion section as future research.

We can approximate a multivariate Gaussian distribution using first and second moments with an appropriate matrix V similar to the homogeneous case. The moment vector M_t for the differential Eqs. (12) and (13) is as follows:

$$M_t = \left(m_{B,t}, m_{R,t}, m_{B^2,t}, m_{R^2,t}, m_{BB,t}, m_{RR,t}, m_{BR,t}\right)^{\mathrm{T}} \tag{14}$$

where M_t is a column vector with the size $\left(\frac{M^2+N^2+3M+3N+2MN}{2} \times 1\right)$, and each element in Eq. (14) is explained in Appendix 2. For example, Eq. (15) shows the moment vector M_t for the $M = N = 2$ case.

$$\begin{aligned}M_t = (\mathrm{E}[B_1], \mathrm{E}[B_2], \mathrm{E}[R_1], \mathrm{E}[R_2], \mathrm{E}\left[B_1^2\right], \mathrm{E}\left[B_2^2\right], \mathrm{E}\left[R_1^2\right], \mathrm{E}\left[R_2^2\right], \\ \mathrm{E}[B_1B_2], \mathrm{E}[R_1R_2], \mathrm{E}[B_1R_1], \mathrm{E}[B_1R_2], \mathrm{E}[B_2R_1], \mathrm{E}[B_2R_2])^{\mathrm{T}}\end{aligned} \tag{15}$$

We use two simple numerical examples to demonstrate how the approximated distribution is similar to the true distribution obtained from the Monte Carlo simulation. We assume that the Monte Carlo simulation result with sufficient time converges to the true distribution. In this paper, we use a CPU i5-2500 (memory = 4 GB) computer for the hardware and a MATLAB R2014b for the software.

2.1. Experiment setting 1 (homogeneous case)

$$B_0 = 100,\ R_0 = 80,\ b = 01,\ r = 0.12$$

First experiment setting 1 is the homogeneous case; the blue and red forces each have only one type of weapon system. The initial strength of the blue force is 100, and the red force is 80. The strength of the red force is 20% less than that of the blue force, but the attrition rate of the red force is (0.12); 20% higher than that of the blue force (0.1).

The joint distribution of each force with the experiment setting 1 at time $t = 5$ is plotted in Figure 1. The left figure shows the simulation result, and the right figure shows the Gaussian approximation obtained by the moment-matching scheme. Since we matched up to 2nd moments, the mean vector and the covariance matrix are the same with the original stochastic process. We approximated the unknown bell-shaped unimodal distribution to Gaussian; obviously, there is a slight difference as we can see in Figure 1. However, it seems to be similar with the human eye.

Hence, we applied statistical hypothesis testing concerning normality. It is truly obvious that the true distribution is not a Gaussian distribution, but we can get an intuition from this hypothesis test that the approximation is reasonable. The null hypothesis is that the samples from the true distribution can be interpreted as samples from a Gaussian distribution, whereas the alternative hypothesis indicates that these samples cannot be interpreted as samples from a Gaussian distribution. In our first try, we randomly sampled 1000 samples from the true distribution and used Henze–Zirkler's multivariate normality test (Henze and Zirkler, 1990). The resulting Henze–Zirkler's statistics was 0.0943, which does not reject the null hypothesis at the significance level at 0.05. Since we sampled randomly, there were some uncertainties that 1000 samples were not enough to represent the true distribution well. We sampled with 10,000 sample sizes 100 times; only 22% of all the hypothesis tests did not reject the null hypothesis. However, with these hypothesis test results, we can carefully say that the true distribution is fairly similar with Gaussian. Justification for the Gaussian assumption will be discussed at the end of the next section, *Battle-end approximation*.

Therefore, we can ensure that the approximated distribution is good enough to describe the true distribution. A Monte Carlo simulation takes about 20 min to get the joint distribution of specific time t with a small time fraction $\mathrm{d}t = 10^{-6}$, whereas the approximation method takes 0.12 s and gives a very similar distribution. If the size of each force gets bigger, the simulation takes much longer to get the exact distribution. However, the approximation method does not depend on the size of the forces and can handle a very large number of troops effectively.

Most actual battles are stochastic, and forces are heterogeneously armed. In many previous researches, however, it was hard to get a good distributional solution that could substitute the simulation because it is not tractable if we build a complex model. As we mentioned before, the proposed approximation provides a remarkable computational benefit by assuming the distribution as Gaussian.

Experiment setting 2 is a heterogeneous case in which each force has two different types of weapon systems. Since there are two types for each force, the initial strengths of each force become vectors denoted in bold face. Similarly, the attrition rates now take a matrix form. For example, b_{12}, which is an (1, 2) element of the attrition rate matrix $\mathbf{b}$, denotes the attrition rate of a 1st type of blue force hitting a 2nd type of red force. We used the 2-type versus 2-type case to demonstrate the joint distributions of each type of force as a 2-dim figure. As mentioned before, in this paper we assume a fixed fire allocation; adaptive fire allocation will be discussed in the conclusion section as future research.

2.2. *Experiment setting 2 (heterogeneous case)*

$$\mathbf{B}_0 = \begin{bmatrix} 100 \\ 30 \end{bmatrix}, \ \mathbf{R}_0 = \begin{bmatrix} 60 \\ 80 \end{bmatrix},$$
$$\mathbf{b} = \begin{bmatrix} 0.08 & 0.12 \\ 0.15 & 0.08 \end{bmatrix}, \ \mathbf{r} = \begin{bmatrix} 0.15 & 0.04 \\ 0.08 & 0.12 \end{bmatrix},$$

Since there are 4 random variable $(B_{1,t}, B_{2,t}, R_{1,t}, R_{2,t})$, it is hard to visualize the joint distribution pictorially. Figure 2 shows the joint distribution of aggregated forces with experiment setting 2 at time $t = 3$. The aggregated force is the sum of the 1st and 2nd types of each forces. Figure 3 shows the 4 joint distributions of all pairs of each force type. The 4 joint distributions on the left side are the results from the

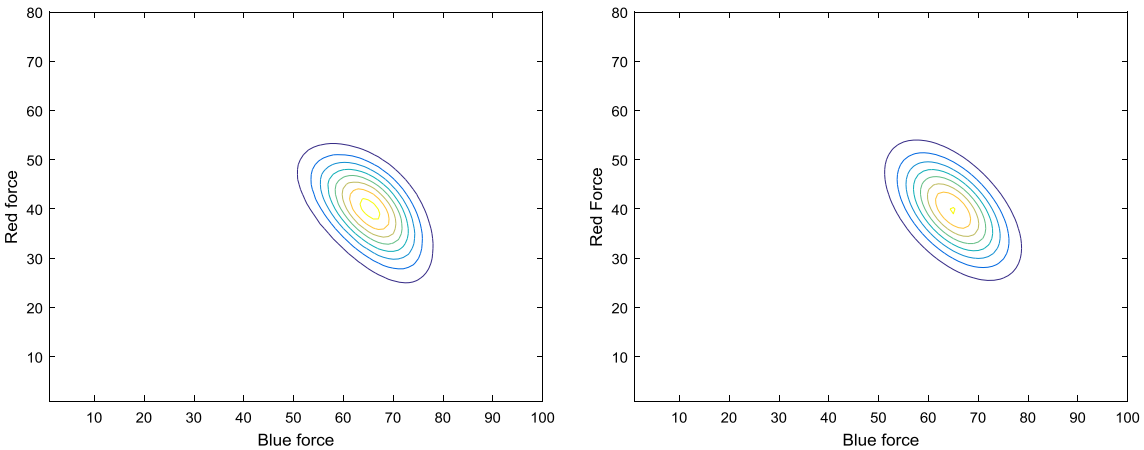

Figure 1 Joint distribution of two forces in the homogeneous case $t = 5$ in experiment setting 1 (*left* simulation, *right* approximation).

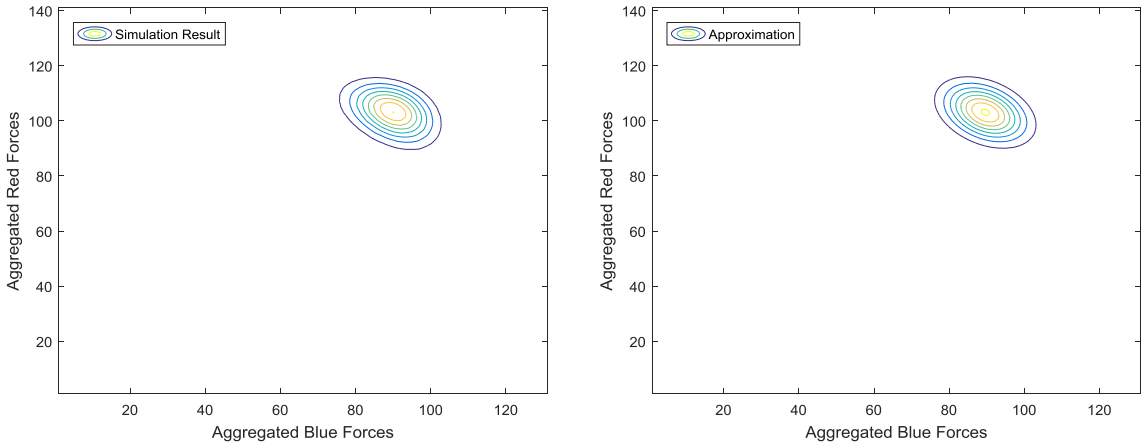

Figure 2 Joint distribution for aggregated forces at $t = 3$ in experiment setting 2 (*left* simulation, *right* approximation).

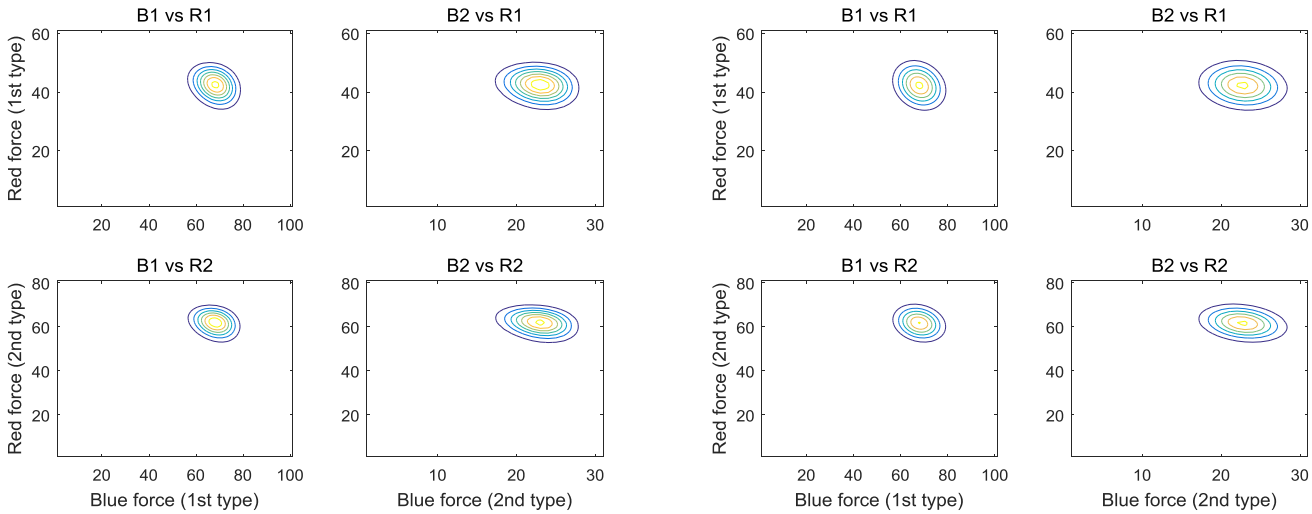

Figure 3 Joint distribution for each pair of forces at $t = 3$ in experiment setting 2 (*left* simulation, *right* approximation).

simulation, and that on the right side are the results from the approximation. Each figure in Figure 3 has subtitles. For example, "B1 versus R1" describes the joint distribution between the 1st type of blue force and the 1st type of red force. Like the homogeneous case, there are obvious slight differences that we can see in Figures 2 and 3. However, the approximation seems good enough to describe the features of the true distribution.

The moment-matching scheme works well in the early and middle phases of warfare, but it starts to break down toward the end of a battle (e.g., $\mathrm{E}[B_t] = 0$). At the end of battle, the simulation or Markovian model does not go under 0 because state transition does not happen. However, this moment-matching method does not restrict a situation wherein B_t and R_t become negative. So, the approximated distribution using the moment-matching scheme becomes different from the simulation result as time progresses, especially at the end of the battle. Therefore, we propose a supporting approximation method called *battle-end approximation*; we use the term *battle-end* to represent the end of a battle.

3. Battle-end approximation

The *moment-matching scheme* mainly concerns the approximation of the joint distribution during a battle, which means the time before battle ends. In this section, we focus on the time close to the end of a battle.

Many previous works on stochastic combat models focused on computing winning (or losing) probability (Lappi *et al*, 2012). However, it is also important to calculate the distribution of survivors for each force type rather because the number of survivors has much more information than just a win or loss (Weale, 1992). It is important to know the survivor distributions of an ally or an enemy at a specific time t in order to analyze the damage or effectiveness of an attack. In this paper,

the situation when a battle is over called the "battle-end" state. This "battle-end" state's probability distribution was not considered or was only able to be obtained with Monte Carlo sampling in previous works. We propose the battle-end approximation method based on the moment-matching scheme.

For the brevity of discussion, we use homogeneous case (hence, 2-dim case) in this section. The result can be easily extended to mixed force cases. Since we are approximating the joint distribution as Gaussian, it is straightforward to compute the probability of battle states as listed in Table 1. If we assume that c is the minimal strength to be able to fight, then the probability can be calculated directly from the Gaussian cumulative distribution function as shown in Table 1, where μ_t and Σ_t are the mean and covariance of the distribution at an arbitrary time t. Here, $\Phi_2([a;b];\mu_t,\Sigma_t)$ denotes the bivariate Gaussian cumulative distribution function with μ_t and Σ_t. For simplicity, we assume that the minimal strength c is equal to 0 for the rest of the paper.

As mentioned earlier, we propose an approximation method to get both the battle-state probability and the distribution of survivors at the "battle-end" state.

Here, T is the time that the red force is defeated (i.e., the event of $T = t$ is the same event as $R_t = 0$). What we are interested in is the distribution of blue force survivors when the red force is defeated: $p(B_T = x)$. By the law of total probability, we get the following equation:

Table 1 Probabilities of battle states for a homogeneous case

Battle States	*Notation*	*Probability*
Both defeated	$P(D_t)$	$\Phi_2([c;c];\mu_t,\Sigma_t)$
Blue wins	$P(B_t)$	$\Phi_2([c;\infty];\mu_t,\Sigma_t) - P(D_t)$
Red wins	$P(R_t)$	$\Phi_2([\infty;c];\mu_t,\Sigma_t) - P(D_t)$
Continues to fight	$P(C_t)$	$1 - P(B_t) - P(R_t) + P(D_t)$

$$p(B_T = x) = \int_0^\infty p(T = t)p(B_t = x|T = t)\mathrm{d}t \tag{16}$$

Equation (16) can be rewritten as:

$p_T(t)$	Probability density function of T
$p_{B_T}(x)$	Probability density function of B_T
$p_{B_T}(x\|T = t)$	Conditional probability density function of B_T

$$\begin{aligned} p_{B_T}(x) &= \int_0^\infty p_T(t)p_{B_T}(x|T = t)\mathrm{d}t \\ &= \int_0^\infty p_T(t)p_{B_T}(x|R_t = 0)\mathrm{d}t \end{aligned} \tag{17}$$

Note that $p_{B_T}(x|R_t = 0)$ is a Gaussian distribution, because it is a conditional distribution of $[B_t, R_t]^{\mathrm{T}}$, which is the bivariate Gaussian random vector. However, the first term $p_T(t)$ is not Gaussian as shown in Eq. (17). Thus, we have to approximate the distribution by calculating the finite difference of $P(T<t)$ with respect to t. By the definition of T, $P(T<t) = P(R_t<0)$, where R_t is the univariate Gaussian. Since calculating $P(R_t<0)$ is trivial, we can numerically approximate $p_T(t)$, and the integration in Eq. (17) can be numerically calculated. This battle-end approximation can be extended to heterogeneous cases.

In the previous section, we proposed the approximation methods applied to a stochastic Lanchester equation, which give the joint distribution of all force components. In this section, we propose the battle-end approximation that supports the moment-matching scheme when the forces become 0 and gives the survivor distribution at the battle-end state.

To demonstrate the suitability of the battle-end approximation, we use the experiment setting 1 with a different time ($t = 10$). The joint distribution of each force with experiment setting 1 at time $t = 10$ is plotted in Figure 4. The left figure shows the simulation result, and the right figure shows

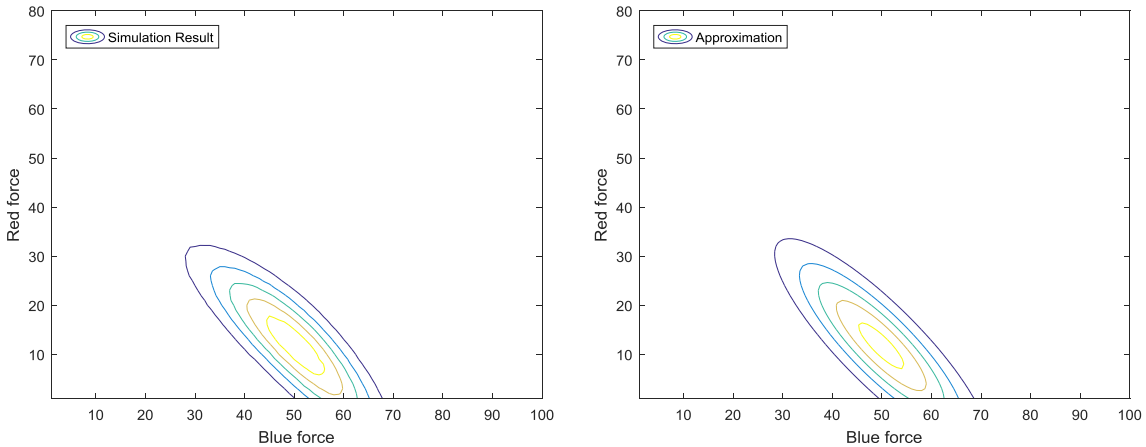

Figure 4 Two joint distributions of each force in the homogeneous case $t = 10$ in experiment setting 1 (*left* simulation, *right* approximation).

the Gaussian approximation obtained by moment-matching and battle-end approximation. Still, both joint distributions seem similar; a notable thing is that both seem to start shrinking to negative. This shrinkage means that there are some probabilities of battle ends with a blue force victory. Actually, the joint distribution does not go under 0 because the battle is stopped at the boundary. Rather than being negative, the probability cumulates on each axis: X axis ($R = 0$) and Y axis ($B = 0$). Figure 5 shows the probability of survivors of the blue forces when the battle ends before $t = 10$, $p(B_T = x|T < 10)$. Figure 5 presents the probability density functions along the X axis ($R = 0$) in Figure 4.

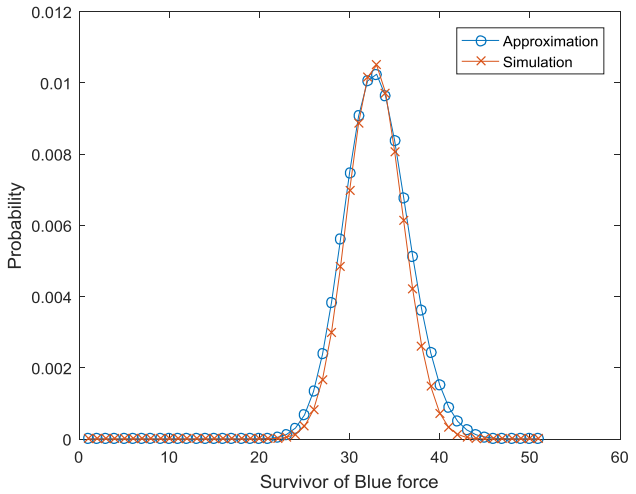

Figure 5 Battle-end state approximation in experiment setting 1.

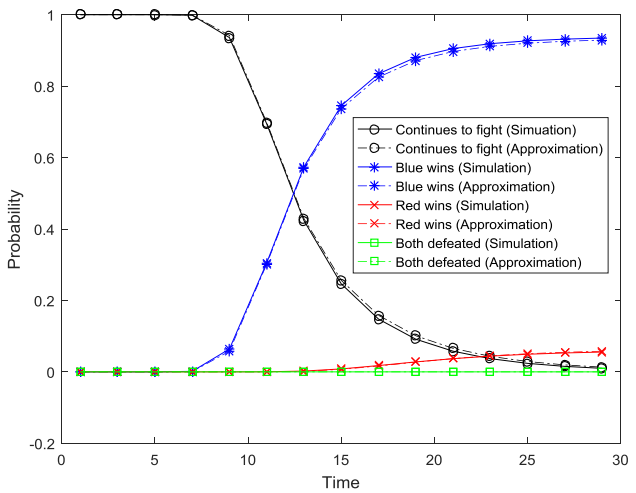

Figure 6 Experiment setting 1: battle-state diagram.

Figure 6 shows a battle-state diagram of experiment setting 1, and each line represents the 4 states specified in Table 1. It shows a similar shape to Lappi *et al* (2012), starting from the *Continues to fight* state and decaying with the rise of *Blue wins* or *Red wins* states. The solid lines represent the state probabilities from the true distribution, and the dotted line represents the approximated distribution. These lines show good matching over time.

For more justification of the Gaussian approximation, we follow the approach of Armstrong (2011), which verifies the stochastic salvo models of naval missile combat as suggested by Armstrong (2005) with various sets of parameter values. We used the similar verification procedure as Armstrong (2011).

Specifically, we generated the scenarios in a wide range to cover various situations in combat, and the scenarios were used as inputs to the approximation and Monte Carlo simulations for comparing their battle outcomes.

We considered the homogeneous case in various situations. The attrition rate of the red force was set to 0.01, and the attrition rate of the blue force varied from 0.05 to 0.15 with an increment of 0.01. Since the attrition rate represents the relative fire power per unit strength of force, we used the same attrition rate parameter set for following numerical experiments, which have different strengths of force. We divided each force strength into 3 cases based on the size listed in Table 2. Like the attrition rate, we fixed the strength of red forces for each case. Since each case had 16 scenarios, we generated a total 528 scenarios (48 cases for the strength of force $\times$ 11 scenarios for the attrition rate).

We compared 3 different measures of fit: the winning probability of the blue force at the end of battle as well as the mean and the standard deviation of the blue force survivors at the end of battle.

Figures 7 and 8 are the numerical results. Figure 7 represents the winning probability of the blue force at the end of battle. Each symbol indicates the type listed in Table 2. As we can see in this figure, the winning probability from the approximation is almost same as that from the simulation. To be more accurate, we conducted a linear regression and got a slope of 1.0034 with an R-squared value nearly 1 and a root-mean-squared error of 0.00588. Hence, we can ensure the Gaussian accurately approximates the true distribution based on the winning probability at the end of the battle. Figure 8 shows the average and the standard deviation of blue force

Table 2 Experiment settings for numerical verification

Type	*Strength of red force*	*Strength of blue force*
Small	10	From 5 to 20 with an increment of 1 (5, 6, …, 20)
Middle	100	From 50 to 200 with an increment of 10 (50, 60, …, 200)
Large	1000	From 500 to 2000 with an increment of 100 (500, 600, …, 2000)

survivors with a log-scaled plot. We can see that it is not as clear as Figure 7. Even though the slopes are 0.9984 and 0.9999 for mean and standard deviation with an R-squared value of nearly 1, some points deviated from the $Y = X$ line. All the experiment settings for these points are "blue overwhelmingly losing" scenarios such as $B = 50$, $R = 100$, $b = 0.05$, and $r = 0.1$. Since we are plotting the properties of blue force survivors, in "blue overwhelmingly losing" scenarios, it seems hard to evaluate the possible blue force survivors because it happens very rarely. Other than these scenarios, all the points are in the $Y = X$ line. One more notable point is that it works quite well even though the troop size is small as shown in Table 2. However, we approximated the original discrete stochastic process as Gaussian, which is the continuous distribution; we thought that at least more than 5 for each force is appropriate for the approximation. Less than 5 for each force would be too small to fit as continuous distribution.

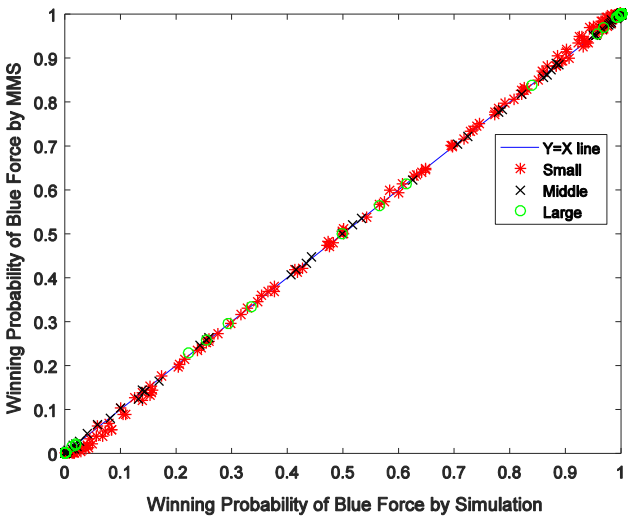

Figure 7 Winning probability of blue force.

4. Applications

Since the moment-matching scheme is a fast and efficient approximation, it can be employed in many applications. In this section, we included 2 application studies: asymmetry force analysis and optimal resource allocation.

In many realistic combat situations, the presence of asymmetric weapon plays critical roles. Hence, analysis based on aggregating asymmetric force into one homogeneous force may result in unrealistic conclusion. The heterogeneously armed force is much more realistic than the homogeneous one, but computational effort grows exponentially as the number of troops and type of weapon systems increase in the Markov chain-type models. However, moment-matching can compute heterogeneously armed forces very fast without aggregating forces to a homogeneous one. Thus, by taking this computational advantage, we can conduct a sensitivity analysis for an asymmetrical heterogeneous force. For example, we can analyze the change of winning probability if we increase the specific type of our forces. These kinds of analyses are hard to conduct with Monte Carlo simulations because of heavy computation, whereas the moment-matching scheme provides an efficient approximate solution.

4.1. Experiment setting 3

$$\mathbf{B} = \begin{bmatrix} 30 \\ 40 \\ 80 \end{bmatrix}, \quad \mathbf{R} = \begin{bmatrix} 84 \\ 135 \\ 70 \end{bmatrix},$$

$$\mathbf{b} = \begin{bmatrix} 0.16 & 0.1 & 0.2 \\ 0.25 & 0.1 & 0.2 \\ 0.25 & 0.1 & 0.16 \end{bmatrix}, \quad \mathbf{r} = \begin{bmatrix} 0.12 & 0.1 & 0.005 \\ 0.1 & 0.08 & 0.005 \\ 0.08 & 0.1 & 0.005 \end{bmatrix}$$

Experiment setting 3 is a good example of an asymmetric heterogeneous force. Blue forces have a smaller number of troops than red forces, but they have a higher attrition rate **b**. Red forces have a larger number of troops than blue forces

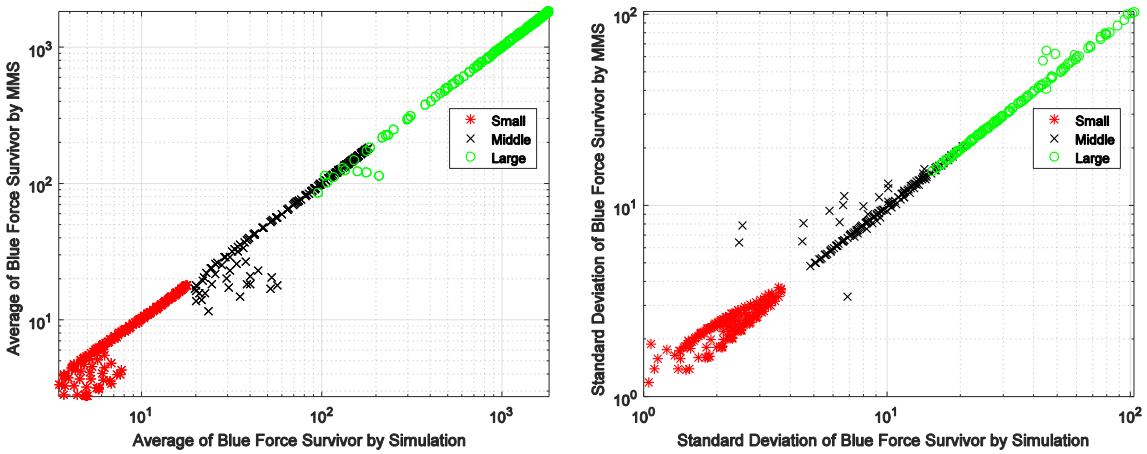

Figure 8 Average (*left*) and standard deviation (*right*) of blue force survivors.

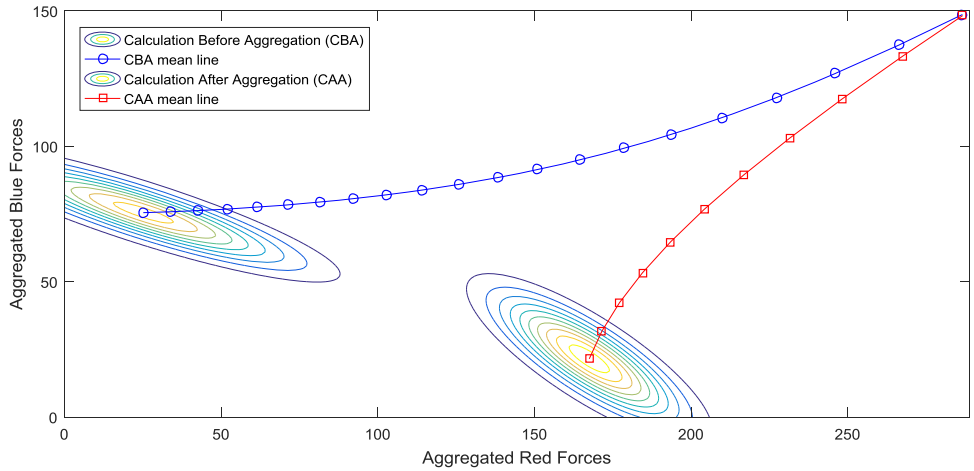

Figure 9 Joint distribution for the asymmetric force case (experiment setting 3) before and after aggregation at $t = 20$.

but have a lower attrition rate **r** and an especially low attrition rate of 0.005 for the 3rd weapon-type of blue forces. In real battle, there would be even more complicated relationships between forces. If we analyzed after aggregating the force into a homogeneous one, these complex interactive relationships would be lost during the aggregation. The aggregation order makes a noticeable difference as seen in Figure 9. If we calculate the joint distribution after aggregation, red forces overwhelm blue forces because the size of red forces is more than twice of blue forces. However, if we calculate the joint distribution before aggregation, blue forces overcome numerical inferiority because of the low attrition rate of 0.005 in **r**.

Calculation after aggregation means aggregating 3 types of each force into a single homogeneous force and calculating the joint distribution of aggregated forces. Naturally, calculation before aggregation means calculating the joint distribution of heterogeneous forces first and aggregating the result. The low attrition rate of the 3rd type of blue forces in **r** is an interesting and remarkable situation in experiment setting 3. If we calculate after aggregation, this condition would not be taken into consideration because we would be summarizing a 3×3 matrix **r** into one constant; so, we should calculate without aggregation. The 3rd type of blue forces represents a difficult opponent-hitting force, such as a sniper on a battlefield situation. The line marked with squares in Figure 9 does not reflect this weapon effect, but the line marked with circles shows that the 3rd type of blue force effectively eliminates all of the red forces as time goes on.

In experiment setting 3, we set $\mathbf{r}_{\cdot 3}$ (the 3rd column of attrition rate **r)** to 0.005 at first, and we observed the battle-state probability change as the value of the 3rd column and the attrition rate varied. The $\mathbf{r}_{\cdot 3}$ means how easily the 3rd type of blue force can be killed by the red forces. If this value increases, then the 3rd type of blue force will be hit more by red forces.

Figure 10 is a diagram that shows the change of battle-state probability as $\mathbf{r}_{\cdot 3}$ varies from 0.001 to 0.03. If this value

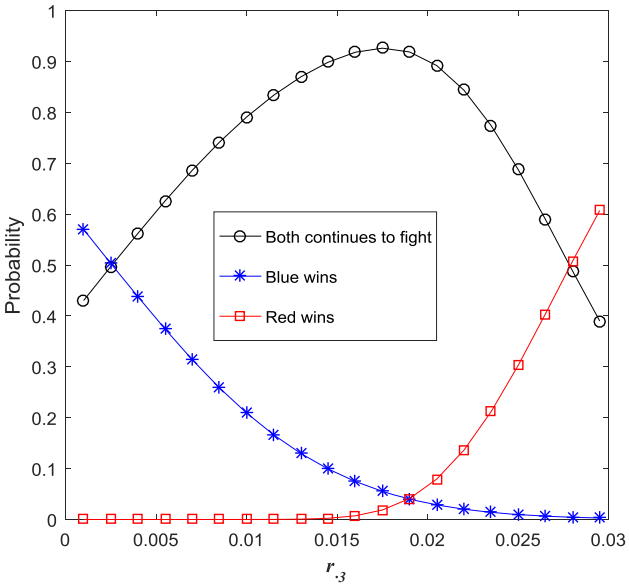

Figure 10 Battle-state probability change as $\mathbf{r}_{\cdot 3}$ at $t = 20$.

decreases, the probability of blue's victory increases. If this value increases, the probability of red's victory increases. This sensitivity analysis is computationally heavier if we use only the simulation. Furthermore, this analysis can be used in an optimal decision-making problem like optimal resource allocation or optimal supply, which leads us to the next application topic.

Another promising application is optimal resource allocation. In this paper, the word *allocation* refers to deciding the composition of forces within a limited budget, not the placement of weapon. Even if all the information is given or known, deciding the optimal composition of our forces against an enemy is not trivial when there are a lot of possible combinations of forces. The number of feasible compositions gets exponentially larger as the number of troops or the budget increases. It is too computationally heavy to compute all the

feasible compositions with simulation. However, our moment-matching helps to compute the joint distribution within a short time and can be applied to modern military systems or complex warfare models, such as network centric warfare. These types of applications will be studied in further research.

5. Conclusion

As modern warfare becomes more complex, newly developed stochastic Lanchester equations also become complex; in the process, it gets intractable and computationally heavy to get a distributional solution. In this paper, we proposed two approximation methods, namely the moment-matching scheme and battle-end approximation, which can approximate a stochastic Lanchester equation solution with a high level of accuracy to the true distribution. This approximation helps to conduct computationally demanding applications like asymmetry force analysis, optimal resource allocation, attrition rate estimation. We also expect that this method can solve much more complex warfare models, such as network centric warfare.

For the heterogeneous case, we assumed a fixed fire allocation in this paper. The optimal fire allocation problem is one of the popular applications of combat modeling, and a relaxation of our approximation algorithm to a non-fixed fire allocation assumption will be a promising subject for further research. One possible way to tackle this problem is to fix the fire allocation for certain small amount of time and do same procedure after we change allocation. Since this method is fast enough, changing the fire allocation certain amount does not affect the computational cost of our method. For example, if we assume there are decision epochs $t_0, t_1, t_2, \ldots$ that the commander can change the fire allocation in each epoch, then we start with the moment vector M_0 and fire allocation π_0 at epoch t_0. After some time, we can get the moment vector M_1 at time t_1 and if the commander changes the fire allocation to π_1, then we start from M_1 to get M_2 at epoch t_2. Continuously varying fire allocation will be another interesting subject for further research.

Acknowledgements—This work was supported by the Defense Acquisition Program Administration and the Agency for Defense Development under the contract UD140022PD, Korea.

References

Amacher M and Mandallaz D (1986). Stochastic versions of Lanchester equations in wargaming. *European Journal of Operational Research* **24**(1):41–45.

Armstrong MJ (2005). A stochastic salvo model for naval surface combat. *Operations Research* **53**(5):830–841.

Armstrong MJ (2011). A verification study of the stochastic salvo combat model. *Annals of Operations Research* **186**(1):23–38.

Bracken J (1995). Lanchester models of the ardennes campaign. *Naval Research Logistics* **42**(4):559–577.

Henze N and Zirkler B (1990). A class of invariant consistent tests for multivariate normality. *Communications in Statistics-Theory and Methods* **19**(10):3595–3617.

Hughes WP (1995). A salvo model of warships in missile combat used to evaluate their staying power. *Naval Research Logistics* **42**(2):267–289.

Karmeshu and Jaiswal NK (1986). A Lanchester-type model of combat with stochastic rates. *Naval Research Logistics Quarterly* **33**(1):101–110.

Kaup GT, Kaup DJ and Finkelstein NM (2005). The Lanchester (n, 1) problem. *Journal of the Operational Research Society* **56**(12): 1399–1407.

Lanchester FW (1916). *Aircraft in warfare: The dawn of the fourth arm*. Constable and Co., Ltd., London.

Lappi E, Pakkanen M and Akesson B (2012). An approximative method of simulating a duel. In *Proceedings of the Winter Simulation Conference*, WSC'12, pp. 1–10.

MacKay NJ (2009). Lanchester models for mixed forces with semi-dynamical target allocation. *Journal of the Operational Research Society* **60**(10):1421–1427.

Taylor JG (1980). *Lanchester-Type Models of Warfare. Volume II*.

Weale TG (1992). Two numerical methods for computing the probability of outcome of a battle of Lanchester type. *The Journal of the Operational Research Society* **43**(8):797.

Appendix 1: Derivation of Eqs. (7)–(9)

$$\begin{aligned}
&\mathrm{E}\Big[(\mathrm{Bern}(rR_t\mathrm{d}t))^2|R_t=R\Big] = 1^2\times\mathrm{P}\Big((\mathrm{Bern}(rR_t\mathrm{d}t))^2=1|R_t=R\Big)\\
&\quad=\mathrm{P}(\mathrm{Bern}(rR_t\mathrm{d}t)=1|R_t=R)=rR\mathrm{d}t\\
&\mathrm{E}\Big[(\mathrm{Bern}(rR_t\mathrm{d}t))^2\Big]=\int_R\mathrm{E}\Big[(\mathrm{Bern}(rR_t\mathrm{d}t))^2|R_t=R\Big]\mathrm{P}(R_t=R)\mathrm{d}R\\
&\quad=\int_R rR\mathrm{d}t\mathrm{P}(R_t=R)\mathrm{d}R\\
&\quad=r\mathrm{d}t\int_R R\mathrm{P}(R_t=R)\mathrm{d}R=r\mathrm{E}[R_t]\mathrm{d}t
\end{aligned}$$

For Eq. 9, it uses the following procedure that gives squared dt.

$$\begin{aligned}
&\mathrm{E}[\mathrm{Bern}(bB_t\mathrm{d}t)\mathrm{Bern}(rR_t\mathrm{d}t)|B_t=B,R_t=R]\\
&\quad=1^2\times\mathrm{P}(\mathrm{Bern}(bB_t\mathrm{d}t)\mathrm{Bern}(rR_t\mathrm{d}t)=1|B_t=B,R_t=R)\\
&\quad=1^2\times\mathrm{P}(\mathrm{Bern}(bB_t\mathrm{d}t)=1|B_t=B)\mathrm{P}(\mathrm{Bern}(rR_t\mathrm{d}t)\\
&\quad=1|R_t=R)=1^2\times bB\mathrm{d}t\times rR\mathrm{d}t=brBR(\mathrm{d}t)^2\\
&\mathrm{E}[\mathrm{Bern}(bB_t\mathrm{d}t)\mathrm{Bern}(rR_t\mathrm{d}t)]\\
&\quad=\int_B\int_R\mathrm{E}[\mathrm{Bern}(bB_t\mathrm{d}t)\mathrm{Bern}(rR_t\mathrm{d}t)|B_t=B,R_t\\
&\quad=R]\mathrm{P}(B_t=B)\mathrm{P}(R_t=R)\mathrm{d}R\mathrm{d}B\\
&\quad=\int_B\int_R brBR(\mathrm{d}t)^2\mathrm{P}(B_t=B)\mathrm{P}(R_t=R)\mathrm{d}R\mathrm{d}B\\
&\quad=br(\mathrm{d}t)^2\int_B\int_R BR\mathrm{P}(B_t=B)\mathrm{P}(R_t=R)\mathrm{d}R\mathrm{d}B\\
&\quad=brE[B_tR_t](\mathrm{d}t)^2
\end{aligned}$$

Appendix 2: First and second moments for a heterogeneous force (*M*-type Blue vs. *N*-type Red)

$$\mathrm{E}\left[B_{i,t+\mathrm{d}t}\right] = \mathrm{E}\left[B_{i,t}\right] - \sum_{k=1}^{N} r_{ki}\mathrm{E}\left[R_{k,t}\right]\mathrm{d}t$$

$$\mathrm{E}\left[R_{j,t+\mathrm{d}t}\right] = \mathrm{E}\left[R_{j,t}\right] - \sum_{l=1}^{M} b_{lj}\mathrm{E}\left[B_{l,t}\right]\mathrm{d}t$$

$$\mathrm{E}\left[B_{i,t+\mathrm{d}t}^2\right] = \mathrm{E}\left[B_{i,t}^2\right] - 2\sum_{k=1}^{N} r_{ki}\mathrm{E}\left[B_{i,t}R_{k,t}\right]\mathrm{d}t + \sum_{k=1}^{N} r_{ki}\mathrm{E}\left[R_{k,t}\right]\mathrm{d}t$$

$$\mathrm{E}\left[R_{j,t+\mathrm{d}t}^2\right] = \mathrm{E}\left[R_{j,t}^2\right] - 2\sum_{l=1}^{M} b_{lj}\mathrm{E}\left[R_{j,t}B_{l,t}\right]\mathrm{d}t + \sum_{l=1}^{M} b_{lj}\mathrm{E}\left[B_{l,t}\right]\mathrm{d}t$$

$$\mathrm{E}\left[B_{i,t+\mathrm{d}t}R_{j,t+\mathrm{d}t}\right] = \mathrm{E}\left[B_{i,t}R_{j,t}\right] - \sum_{l=1}^{M} b_{lj}\mathrm{E}\left[B_{i,t}B_{l,t}\right]\mathrm{d}t - \sum_{k=1}^{N} r_{ki}\mathrm{E}\left[R_{j,t}R_{k,t}\right]\mathrm{d}t$$

$$\mathrm{E}\left[B_{i,t+\mathrm{d}t}B_{j,t+\mathrm{d}t}\right] = \mathrm{E}\left[B_{i,t}B_{j,t}\right] - \sum_{k=1}^{N} r_{ki}\mathrm{E}\left[B_{j,t}R_{k,t}\right]\mathrm{d}t - \sum_{k=1}^{N} r_{ki}\mathrm{E}\left[B_{i,t}R_{k,t}\right]\mathrm{d}t$$

$$\mathrm{E}\left[R_{i,t+\mathrm{d}t}R_{j,t+\mathrm{d}t}\right] = \mathrm{E}\left[R_{i,t}R_{j,t}\right] - \sum_{k=1}^{N} b_{ki}\mathrm{E}\left[R_{j,t}B_{k,t}\right]\mathrm{d}t - \sum_{k=1}^{N} b_{ki}\mathrm{E}\left[R_{i,t}B_{k,t}\right]\mathrm{d}t$$

$$M_t = expm(V)^t M_0$$

$$M_t = \left(m_{B,t}, m_{R,t}, m_{B^2,t}, m_{R^2,t}, m_{BB,t}, m_{RR,t}, m_{BR,t}\right)^{\mathrm{T}}$$

where

$$m_{B,t} = \left(\mathrm{E}\left[B_{1,t}\right], \ldots, \mathrm{E}\left[B_{M,t}\right]\right)$$
$$m_{R,t} = \left(\mathrm{E}\left[R_{1,t}\right], \ldots, \mathrm{E}\left[R_{N,t}\right]\right)$$
$$m_{B^2,t} = \left(\mathrm{E}\left[B_{1,t}^2\right], \ldots, \mathrm{E}\left[B_{M,t}^2\right]\right)$$
$$m_{R^2,t} = \left(\mathrm{E}\left[R_{1,t}^2\right], \ldots, \mathrm{E}\left[R_{N,t}^2\right]\right)$$
$$m_{BB,t} = \left(\mathrm{E}\left[B_{1,t}B_{2,t}\right], \mathrm{E}\left[B_{1,t}B_{3,t}\right] \ldots, \mathrm{E}\left[B_{M-1,t}B_{M,t}\right]\right)$$
$$m_{RR,t} = \left(\mathrm{E}\left[R_{1,t}R_{2,t}\right], \mathrm{E}\left[R_{1,t}R_{3,t}\right] \ldots, \mathrm{E}\left[R_{N-1,t}R_{N,t}\right]\right)$$
$$m_{BR,t} = \left(\mathrm{E}\left[B_{1,t}R_{1,t}\right], \mathrm{E}\left[B_{1,t}R_{2,t}\right] \ldots, \mathrm{E}\left[B_{M,t}R_{N,t}\right]\right)$$

V = $\left(\frac{\mathrm{M}^2 + N^2 + 3M + 3N + 2MN}{2}\right)^2$ Matrix, sorted as M_t

$$V = \begin{pmatrix} \cdot & -\boldsymbol{r}_{\boldsymbol{M}\times\boldsymbol{N}} & \cdot & \cdot & \cdot & \cdot & \cdot \\ -\boldsymbol{b}_{\boldsymbol{N}\times\boldsymbol{M}} & \cdot & \cdot & \cdot & \cdot & \cdot & \cdot \\ \cdot & \boldsymbol{r}_{\boldsymbol{M}\times\boldsymbol{N}} & \cdot & \cdot & \cdot & \cdot & -2\boldsymbol{r}_{\boldsymbol{M}\times\boldsymbol{MN}} \\ \boldsymbol{b}_{\boldsymbol{N}\times\boldsymbol{M}} & \cdot & \cdot & \cdot & \cdot & \cdot & -2\boldsymbol{b}_{\boldsymbol{N}\times\boldsymbol{MN}} \\ \cdot & \cdot & \cdot & \cdot & \cdot & \cdot & -2\boldsymbol{r}_{\frac{(M^2-M)}{2}\times\boldsymbol{MN}} \\ \cdot & \cdot & \cdot & \cdot & \cdot & \cdot & -2\boldsymbol{b}_{\frac{(N^2-N)}{2}\times\boldsymbol{MN}} \\ \cdot & \cdot & -\boldsymbol{b}_{\boldsymbol{MN}\times\boldsymbol{M}} & -\boldsymbol{r}_{\boldsymbol{MN}\times\boldsymbol{N}} & -\boldsymbol{b}_{\boldsymbol{MN}\times\frac{M^2-M}{2}} & -\boldsymbol{r}_{\boldsymbol{MN}\times\frac{N^2-N}{2}} & \cdot \end{pmatrix}$$

V is filled with 12 nonzero submatrices, where $\cdot$ is a 0-filled matrix with a proper size. Here, the subscript for submatrices denotes the size of those matrices. All the submatrices are different, and it can be filled easily with the equations in Appendix 1. For example, V for 2-type blue force versus 2-type red force is as follows: ($M = 2$, $N = 2$).

$$
\mathrm{V} = \begin{pmatrix}
\cdot & & -r_{11} & -r_{21} & \cdot & & \cdot & & \cdot & & \cdot & & & \cdot & & \\
 & & -r_{12} & -r_{22} & & & & & & & & & & & & \\
-b_{11} & -b_{21} & & \cdot & & \cdot & & \cdot & & \cdot & & & & \cdot & & \\
-b_{12} & -b_{22} & & & & & & & & & & & & & & \\
 & \cdot & r_{11} & r_{21} & & \cdot & & \cdot & & \cdot & -2r_{11} & -2r_{21} & 0 & 0 & & \\
 & & r_{12} & r_{22} & & & & & & & 0 & 0 & -2r_{12} & -2r_{22} & & \\
b_{11} & b_{21} & & \cdot & & \cdot & & \cdot & & \cdot & -2b_{11} & 0 & -2b_{21} & 0 & & \\
b_{12} & b_{22} & & & & & & & & & 0 & -2b_{12} & 0 & -2b_{22} & & \\
\cdot & & \cdot & & \cdot & & \cdot & & \cdot & & -r_{12} & -r_{22} & -r_{11} & -r_{21} & & \\
\cdot & & \cdot & & \cdot & & \cdot & & \cdot & & -b_{12} & -b_{11} & -b_{22} & -b_{21} & & \\
 & & & & -b_{11} & 0 & -r_{11} & 0 & -b_{21} & -r_{21} & & & & & & \\
 & \cdot & & \cdot & -b_{12} & 0 & 0 & -r_{21} & -b_{22} & -r_{11} & & & & \cdot & & \\
 & & & & 0 & -b_{21} & -r_{12} & 0 & -b_{11} & -r_{22} & & & & & & \\
 & & & & 0 & -b_{22} & 0 & -r_{22} & -b_{21} & -r_{12} & & & & & &
\end{pmatrix}
$$

Received 21 March 2016;
accepted 28 November 2016